UC Davis
UC Davis Previously Published Works

Title

Topical treatment of tyrosine kinase 2 inhibitor through borneol-embedded hydrogel: Evaluation for preventive, therapeutic, and Recurrent management of psoriasis.

Permalink

https://escholarship.org/uc/item/95m2h6rk

Authors

Lai, Yuhsien

Wu, Xuesong

Jiang, Zhuoyu

et al.

Publication Date

2024-11-01

DOI

10.1016/j.bioactmat.2024.07.013

Copyright Information

Peer reviewed
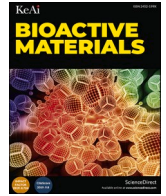
Topical treatment of tyrosine kinase 2 inhibitor through borneol-embedded hydrogel: Evaluation for preventive, therapeutic, and Recurrent management of psoriasis

Yuhsien Lai [a], Xuesong Wu [b], Zhuoyu Jiang [a], Yifei Fang [c], Xiuting Liu [a], Dan Hong [a], Yanyun Jiang [a], Guozhen Tan [a], Shiqi Tang [d], Siyao Lu [a], David Wei [b], Sam T. Hwang [b], Kit S. Lam [d], Liangchun Wang [a], Yanyu Huang [d,*,1], Zhenrui Shi [a,**,1]

[a] *Department of Dermatology, Sun Yat-sen Memorial Hospital, Sun Yat-sen University, 510120, China*
[b] *Department of Dermatology, University of California-Davis, Sacramento, CA, 95817, USA*
[c] *School of Biomedical Engineering, Sun Yat-sen University, 518107, China*
[d] *Department of Biochemistry and Molecular Medicine, University of California-Davis, Sacramento, CA, 95817, USA*

ARTICLE INFO

ABSTRACT

Psoriasis, an immune-mediated inflammatory skin disorder characterized by a chronically relapsing-remitting course, continues to be primarily managed through topical therapy. While oral administration of tyrosine kinase 2 inhibitors (TYK2i) stands as an effective approach for psoriasis treatment, the potential efficacy of topical application of TYK2i remains unexplored. Herein, the carbomer/alginic acid hydrogel is embedded with borneol (BO) as a new topical carrier of TYK2i for achieving enhanced transdermal permeation and anti-psoriasis efficacy. The hydrogel system, *i.e.*, TYK2i-BO-gel, exhibits significantly improved preventative and therapeutic effects in mice models of psoriasiform dermatitis, as evidenced by phenotypical images, psoriasis severity score index (PSI), histology, immunohistochemical staining, and PCR analysis. Remarkably, TYK2i-BO-gel outperforms conventional topical corticosteroid therapy by significantly preventing psoriatic lesion recurrence as measured by a nearly 50 % reduction in ear thickness changes ($p < 0.0001$), PSI ($p < 0.0001$) and epidermal thickness ($p < 0.05$). Moreover, a strengthened anti-inflammatory effect caused by TYK2i-BO-gel is seen in a human skin explant model, implying its potential application for human patients. With the addition of BO, the TYK2i-BO-gel not only increases skin permeability but also inhibits the expression of antimicrobial peptides in keratinocytes and facilitates the anti-Th17 response of TYK2i with suppressed activation of STAT3. Therefore, this work represents the accessibility and effectiveness of TYK2i-BO-hydrogel as a new topical formulation for anti-psoriasis management and shows great potential for clinical application.

1. Introduction

Psoriasis is a common, chronic papulosquamous skin disease that affects 2–3% of the global population and substantially burdens individuals and society [1]. While the exact causes of psoriasis are not fully understood, it is known to be an autoimmune disease with a strong genetic component that environmental factors, including drugs, can trigger. The dysfunction of epidermal keratinocytes provoked by immune cells, particularly T cells and their related immune mediators such as interleukin (IL)-23 and IL-17A, has been identified as the key process of psoriasis pathogenesis [2]. Many treatment options are available to help manage the symptoms of psoriasis, but there is currently no cure for the condition [3].

Topical administration is a convenient route for delivering therapeutic agents. Specifically, topical drug delivery systems are crafted to exert targeted therapeutic effects on one or multiple skin layers without

medical intervention, making them particularly compatible with addressing conditions like psoriasis. Clinically, mild psoriasis can often be managed with topical agents, while patients with moderate to severe disease may need phototherapy or systemic therapy in combination with some topical agents [4]. Therefore, topical drugs remain the mainstay for treating psoriasis, especially for localized lesions that account for the majority of the psoriasis population. Glucocorticosteroids, vitamin D derivatives, and retinoids are the topical agents predominantly used as conventional therapies for treating psoriasis [4]. However, they have adverse effects, such as skin irritation, hypertrichosis, and atrophy. More importantly, the common challenge for psoriasis treatment, including conventional therapies, many newly approved biologics, and small-molecule drugs, is recalcitrant lesions and disease recurrence after drug withdrawal. Therefore, the rational design of a topical formulation with high biocompatibility to the skin and a prolonged drug release profile in the foci is urgently desired for anti-psoriasis treatment.

Janus kinase (JAK) inhibitors block the intracellular signal pathway mediated by JAK and signal transducer and activator of transcription (STAT) proteins, thereby inhibiting gene transcription of pro-inflammatory cytokines [5]. These inhibitors are already on the market for rheumatoid arthritis, psoriatic arthritis (PsA), and ulcerative colitis [6], and also showed great potential in treating psoriasis [7]. Among all known JAK members, TYK2 is mainly responsible for the regulation of pro-inflammatory, pro-immune signal transduction and cell response driven by IL-23, IL-12, and type I interferons (IFNs), which are all key pathogenic cytokines in the development and maintenance of psoriasis, thus making TYK2 an attractive target of treating autoimmune and inflammatory diseases with higher efficacy [8]. BMS-986165 is a newly developed oral TYK2 inhibitor (TYK2i) that similarly blocks receptor-stimulated activation of TYK2 allosterically with high selectivity and potency afforded through optimized binding to a regulatory domain of the protein [9]. Previous clinical trials have demonstrated that BMS-986165 is superior to placebo in moderate to severe psoriasis [10]. A very recent study further explored the efficacy of topical brepocitinib cream, a TYK2/JAK1 inhibitor in mild to moderate psoriasis, but failed to observe any statistically significant improvement in patients treated with brepocitinib cream versus the vehicle group [11]. Therefore, novel formulations and solutions to improve the efficacy of topical TYK2i and potentially other JAK inhibitors to treat psoriasis are urgently needed.

Hydrogels represent intricate three-dimensional polymeric networks with unique adhesive properties, semi-solid consistency, swelling attributes, and biocompatibility [12]. These hydrogels possess a mesh-like matrix structure, wherein the cross-linking density can be enhanced through the thickening agents. This enhancement holds the potential to finely tune drug release kinetics and skin permeation patterns [13]. Among different hydrogel matrices, carbomer-based formulations find diverse applications in the medical and cosmetic realm, primarily in the application of topical gels and creams for wound dressings or sunscreens [14]. Additionally, carbomer-based gels serve as carriers for the transport of specific medications through the skin or mucus to yield localized or systemic therapeutic outcomes [15]. On the other hand, alginic acid-based hydrogels, derived from brown *algae*, have gained attention for their versatility in the application of controlled-releasing drugs [16]. This strategy has been explored in diverse areas, such as wound healing [17], transdermal drug delivery [18], and anti-infection [19]. Moreover, alginic acid has shown anti-inflammatory effects in keratinocytes and dermal fibroblasts, raising the potential of alginic acid in treating inflammatory skin disorders like psoriasis [20].

Borneol (BO) is a natural terpene found in many plants, including camphor trees and mint species. It has been used in traditional medicine for thousands of years and is known for its anti-inflammatory, analgesic, and anti-bacterial properties [21]. BO has shown the potential to treat a wide range of medical conditions, including infection, neurological, cardio-cerebrovascular diseases, and cancers [22]. Regarding skin disorders, BO has significant anti-inflammatory effects on acne enhancing

its healing by increasing the collagen generation combined with photodynamic therapy [23]. In addition to its therapeutic properties, BO has been used as a natural penetration enhancer in topical formulations [24].

In this study, we designed a carbomer/alginic acid-based hydrogel formulation loading BMS-986165, on the skin to treat psoriasis. For the first time, we integrated BO into a TYK2i-loaded hydrogel system and showed that the formulation achieved enhanced therapeutic effects on imiquimod (IMQ)-induced psoriatic mice with significantly reduced scaling and erythema, leukocyte infiltration, and expression of proinflammatory cytokines. More importantly, the compound formulation of BO and TYK2i showed comparable efficacy with potent topical steroids and additionally prevented skin inflammation relapse upon IMQ rechallenge. Consistently, the superiority of BO plus TYK2i in inhibiting inflammation was confirmed in skin explants from psoriasis patients. BO suppressed the expression of antimicrobial peptides (AMPs) in keratinocytes, facilitated the anti-T helper (Th) 17 response of TYK2i, and increased skin permeability, which contributed to the enhanced therapeutic effects. The significant results in this study, especially the data from mice models and *in vitro* skin culture, suggest the great translational potential of BO and TYK2i-loaded hydrogel for clinical application to psoriasis (Scheme 1).

2. Results and discussion

2.1. Topical hydrogel formulation of TYK2i is superior in treating psoriasiform dermatitis (PsD) of IMQ mice

Although the efficiency of oral TYK2i, BMS-986165, has been demonstrated for psoriasis, its potential as a topical therapy has not been explored. We first assessed the potential of topical administration of TYK2i by simply dissolving it in corn oil, a widely used vehicle for transdermal delivery [25]. IMQ, a ligand of Toll-like receptors (TLR) 7 and 8, has been reported to induce dermatitis in mice and other animals, capitulating several important aspects of human psoriasis [26]. In prior studies, skin thickness measurements, psoriasis severity index (PSI) score, histological staining, splenic involvement, infiltration of immune cells, and production of inflammatory cytokines have been very well established as measures of inflammation in this model. It has already been successfully exploited for the screening of various conventional topical formulations and novel drug nanovectors [27]. We then utilized this model to evaluate the effects of topical TYK2i in a preventative manner. As illustrated in Fig. 1A, corn oil containing TYK2i (0.1 %, weight/weight %) and IMQ were applied individually over the ear skin by following the schedule, i.e., corn oil TYK2i was administered in the morning and afternoon, twice a day, while IMO was separately applied at noon so they were not mixed. The concentration of TYK2i was based on the fact that cream of brepocitinib, a selective inhibitor of TYK2/-JAK1, did not show superiority in treating psoriasis when applied at 3 % versus 0.1 % [11]. The psoriatic skin inflammation induced by IMQ was characterized by typical manifestations of erythema, thickening, and scaling, which was mildly attenuated in mice treated with corn oil containing TYK2i (Fig. 1B). The treatments led to a partial reduction in ear thickness (mean $\pm$ SEM: 0.45 $\pm$ 0.019 mm vs.0.37 $\pm$ 0.008 mm, p = 0.01) and PSI scores (mean $\pm$ SEM: 5.62 $\pm$ 0.18 vs.4.66 $\pm$ 0.33, p = 0.02) (Fig. 1C) and a slight decrease in epidermal thickness (mean $\pm$ SEM: 48.97 $\pm$ 2.77 μm vs.40.35 $\pm$ 0.77 μm, p = 0.02) (Fig. 1D and E). Although there is moderate improvement in epidermal hyperplasia, the nuclear staining of Ki-67 (a marker of cell proliferation) [24] in the epidermis did not differ between the two groups of mice (Fig. 1F). Histological analysis showed a 55 % decrease in Munro microabscesses (a microscopic collection of neutrophils in the stratum corneum (SC) of the epidermis) in the TYK2i-treated mice (p = 0.02) (Fig. 1G). Similarly, an approximately 50 % reduction in the transcripts of several psoriasis-related markers, including *Il1b*, *Il6*, and *Cxcl2*, and antimicrobial peptides (AMPs), including *S100a8* and *S100a9* were observed by
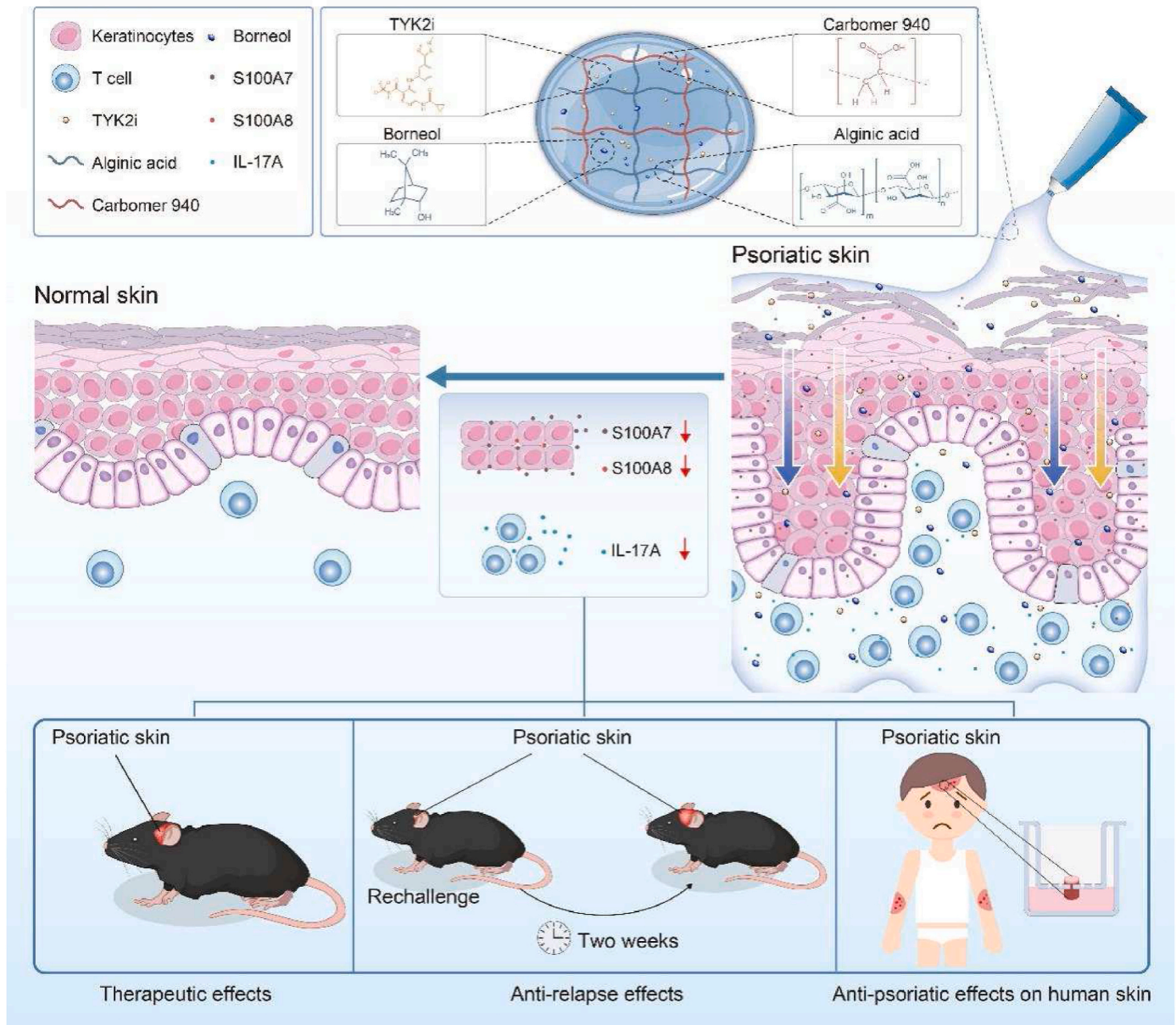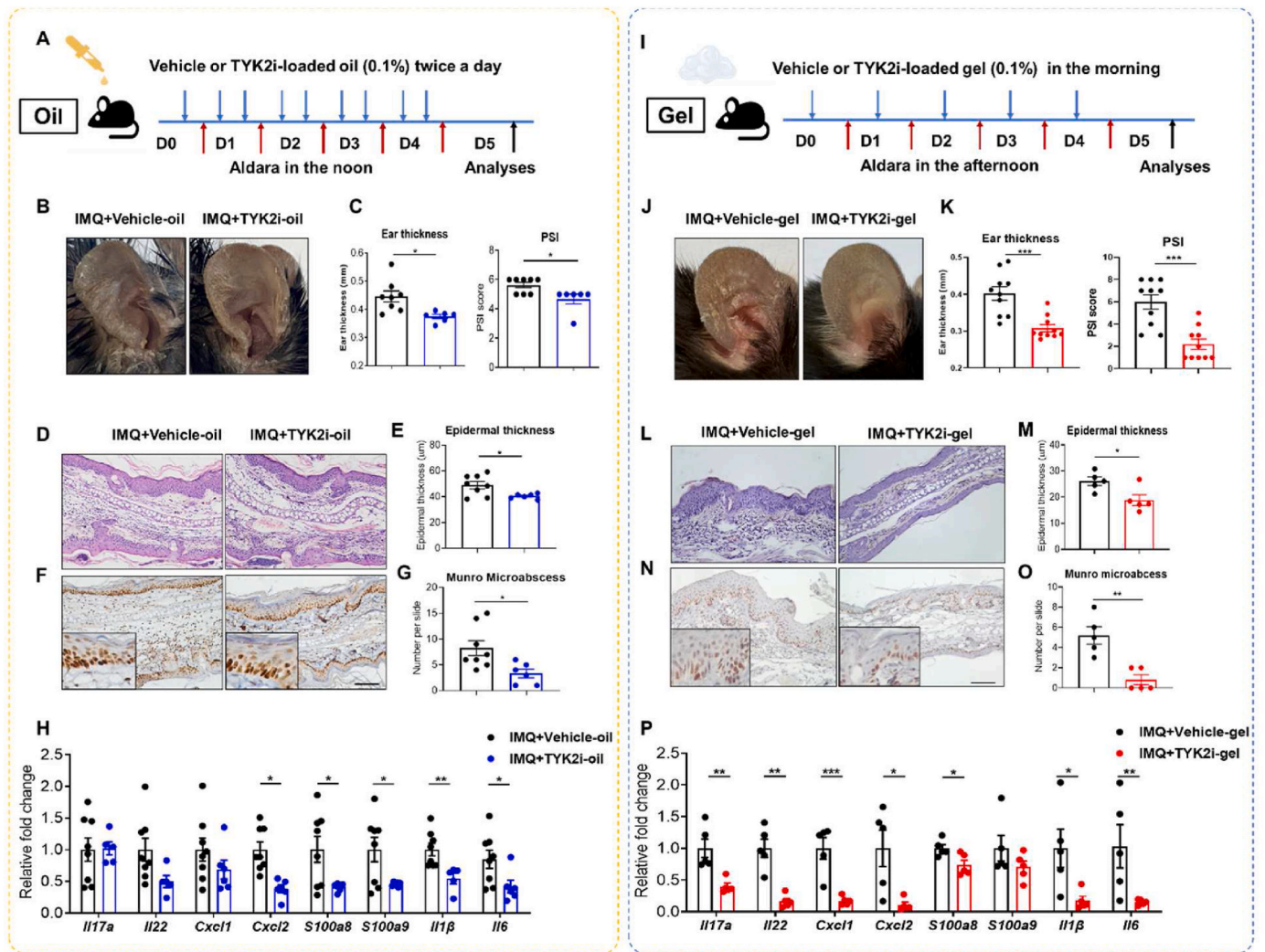
Scheme 1. Schematic illustration of the preparation of TYK2i-BO-gel and its mechanism for treatment in mouse models and a human skin explant model.
The carbomer/alginic acid hydrogel was embedded with BO as a new topical carrier of TYK2i. The effectiveness of TYK2i-BO-gel was demonstrated in in (1) a therapeutic mice model of PsD where skin inflammation was established before initiating treatment; (2) a relapse mice model of PsD where skin inflammation was exacerbated after rechallenge of stimulus; (3) a human skin explant model from psoriatic lesion. The superior effectiveness of TYK2i-BO-gel was associated with increased skin permeability by adding BO, inhibited expression of AMPs in keratinocytes, and Th17 response by the combined use of TYK2i and BO.

RT-PCR (Fig. 1H). However, corn oil containing TYK2i did not affect cytokines, such as Th17 cytokines (*Il17a*, *Il22*) and a key neutrophil chemoattractant (*Cxcl1*), the key players in psoriasis. These results suggest that the TYK2i applied in corn oil formulation has a moderate preventive effect against IMQ-induced PsD.

To enhance the therapeutic effect of TYK2i in oil, we set out to design an advanced topical formulation for TYK2i. The commonly used topical formulations for treating psoriasis include ointment, cream, emulsion, and hydrogel, among which hydrogel holds unique superiority, such as better transdermal penetration, moisturizing properties, and comfort to be used in hair-covered areas (scalp psoriasis). A natural anionic polysaccharide, alginic acid, and its salts, e.g., sodium alginate, have been intensively used as pharmaceutical ingredients for diverse biomedical applications due to their anti-inflammatory features and considerable biocompatibility [20a]. Herein, we developed a hydrogel formulation using alginic acid and Carbopol 940 polymer (a carbomer widely used thickening agent that helps control the viscosity and rheology of cosmetic products) at a 4:1 ratio, which was modified on a formulation previously demonstrated superiority for topical administration [28].

Triethanolamine (TEA) was added to neutralize carbomer because the gelling action of Carbopol 940 would be triggered at pH 6. Vehicle or TYK2i-loaded hydrogel was applied daily on the ear in the morning, and IMQ was applied at noon (Fig. 1I). As a result, mice treated with TYK2i-gel did not exhibit weight loss relative to those with vehicles (data not shown), yet daily application of TYK2i-gel significantly reduced erythema, scaling, ear swelling (mean $\pm$ SEM: 0.40 ± 0.018 mm vs.0.30 ± 0.010 mm, $p = 0.0003$), and PSI score (mean $\pm$ SEM: 6.0 ± 0.65 vs.2.2 ± 0.47, $p = 0.0002$) (Fig. 1J and K). H&E staining further revealed that TYK2i-gel-treated mice had more than a 40 % decrease in epidermal hyperplasia ($p = 0.025$) (Fig. 1L and M), and the immunohistochemistry

Fig. 1. Topical gel formulation of TYK2 inhibitor exerts superior efficacy than corn oil formulation in treating psoriasiform dermatitis (PsD). (A) Schematic illustration of experimental protocols: WT C57BL/6 mouse ears were topically treated with corn oil (vehicle) or deucravacitinib (TYK2 inhibitor, TYK2i) dissolved in corn oil (w/w 0.1 %) every day in the morning and the afternoon, with imiquimod (IMQ) at noon; (B) Representative photographs, (C) ear thickness and Psoriasis severity index (PSI) score, (D) image of H&E section, (E) analysis of epidermal thickness, (F) immunohistochemical (IHC) staining of Ki-67, (G) number of microabscesses, and (H) gene expression of psoriasis-related markers in the ear skin. (I) Schematic illustration of experimental protocols: mouse ears were topically treated with vehicle or TYK2i-loaded gel (w/w 0.1 %) every day in the morning with IMQ in the afternoon: (J) Representative photographs, (K) ear thickness and PSI score, (L) image of H&E section, (M) analysis of epidermal thickness, (N) IHC staining of Ki-67, (O) number of microabscesses, and (P) gene expression of psoriasis-related markers in the ear skin. All the data are presented as mean ± SEM. Four to five mice per group. At least two independent experiments were performed for data analysis *in vivo*. Scale bar, 100 μm *$p < 0.05$, **$p < 0.01$, ***$p < 0.001$, by using two-tailed Student's t-test.

(IHC) results showed noticeably weaker staining of Ki-67 in the ear section after treated with TYK2i-loaded hydrogel (Fig. 1N). What's more, there were approximately 75 % fewer Munro microabscesses in mice treated with TYK2i-gel than those in vehicle-treated mice ($p = 0.002$) (Fig. 1O). The treatment of TYK2i-hydrogel also led to fewer cell counts of cervical lymph nodes (cLNs) and a lesser extent of spleno-megaly (Fig. S1), demonstrating that the hydrogel formulation of TYK2i improved the systemic inflammation. Consistent with these results, flow cytometric analysis showed that both the percentage and absolute number of neutrophils in the ear skin were reduced by the treatment of TYK2i-hydrogel (Fig. S2A).

There are two distinct subsets of γδ cells in mice skin discriminated by the T-cell receptor (TCR) present on the cell surface: γδ-high expressing T cells (also known as dendritic epidermal T cells, DETC) and γδ-low expressing T cells (DETC are TCR-bright whereas the γδ-low T cell are found to be TCR-intermediate). In our previous work, we demonstrated that γδ-low T cells account for a majority of IL-17A pro-duction and are required to develop full-blown skin inflammation in an

IL-23 injection PsD model [29]. In this study, we found that fewer counts of γδ-low T cells were seen in TYK2i-treated mice than those in the vehicle-treated mice, as shown in the flow cytometry analysis in Fig. S2B. In contrast to the ear skin treated with corn oil containing TYK2i, those treated with TYK2i-gel showed a significant suppression in mRNA levels of *Il17a* (fold change, mean ± SEM: 1.0 ± 0.15 vs.0.40 ± 0.05, $p = 0.0022$), *Il22* (fold change, mean ± SEM: 1.0 ± 0.15 vs.0.17 ± 0.045, $p = 0.0006$), and *Cxcl1* (fold change, mean ± SEM: 1.0 ± 0.17 vs.0.17 ± 0.03, $p = 0.0012$) (Fig. 1P). Moreover, TYK2i-loaded gel also resulted in profound decreases in the expression of *Il1b*, *Il6*, and *S100a8* compared to the vehicle hydrogel. These data collectively demonstrate that the TYK2i in hydrogel formulation exhibits superior potential for treating psoriasis compared to its counterpart in corn oil.

### 2.2. Preparation and characterization of TYK2i-BO-loaded hydrogel

Drug permeability is a critical factor for maximizing the treatment effect of a topical medicine. The above hydrogel formation may not be

effective in penetrating the skin barrier to reach its target, and thus, the TYK2i effects will be hampered. In this study, we introduced BO, a permeability enhancer that can be extracted from various medicinal plants, into the hydrogel system. BO has been shown to perturb the structure of SC lipids and improve drug penetration through the skin [24]. As illustrated in Fig. 2A, TYK2i and BO were loaded in the alginic acid/carbomer-based hydrogel. Both vehicle-gel and TYK2i-BO-loaded hydrogel retained their shape and consistency at the bottom of the tube when they were placed upside down, while the hydrogel solution that did not contain TEA as a neutralizing reagent existed in a flow state (Fig. 2B). Next, scanning electron microscopy (SEM) was used to visualize the morphology of the as-prepared hydrogel. As observed in SEM images, both vehicle- and TYK2i-BO-loaded hydrogel contained numerous pores interconnected to each other in the structures. In particular, the loading of TYK2i and BO in the hydrogel networks

showed smaller size pores compared to vehicle-gel, which are expected to facilitate stronger mechanical strength.

Next, the thermogravimetric analysis (TGA) was performed to characterize the composition of the as-prepared hydrogel. As shown in Fig. S3, both Vehicle-gel and TYK2i-BO-gel exhibited a similar declining trend in mass. Specifically, the mass of both hydrogel formulations dropped by 10 % at around 100 °C significantly due to the evaporation of water. With the enhancement of temperature (~200–300 °C), a 50 % mass was lost owing to the burning and decomposition of carbomer, alginic acid, BO, and TYK2i. This data suggested that TYK2i-BO- gel maintained its structural integrity at ambient temperatures, which would enhance its potential for maintaining biological activity during topical administration.

Furthermore, the structural information of the TYK2i-BO-gel was revealed by Fourier-transform infrared spectroscopy (FTIR, Fig. S4). In
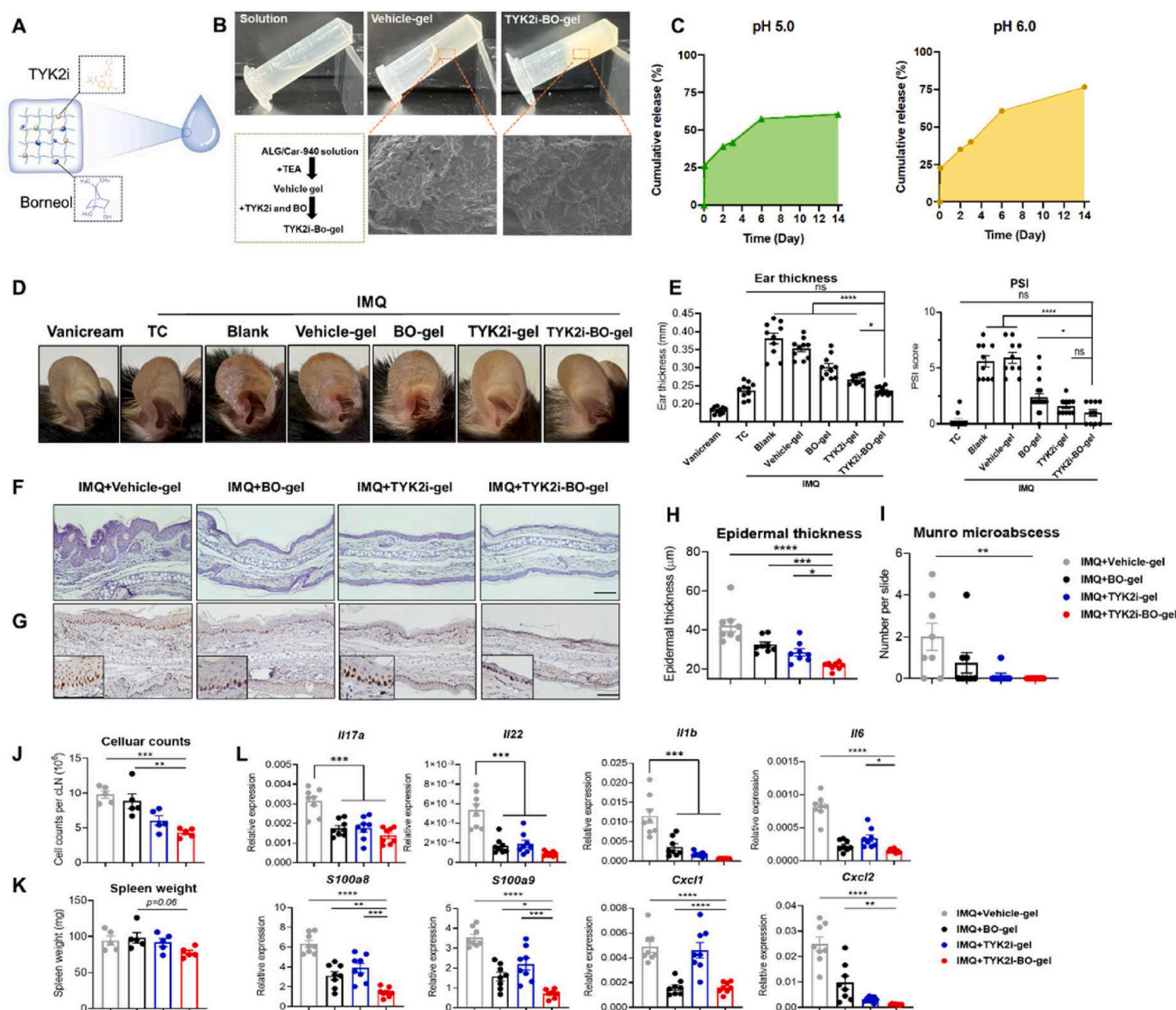
Fig. 2. Topical application of BO and TYK2i in combination effectively improves PsD. (A) Schematic illustration of the formation of TYK2i-BO-gel. (B) Presentative photographs and SEM images of vehicle-gel and TYK2i-BO-gel, scale bar = 100 μm. (C) Release rate of TYK2i from TYK2i-BO-gel in PBS at pH 5.0 and pH 6.0 by 14 days of incubation. Mouse ears were given indicated treatment every day in the morning with vanicream or IMQ in the afternoon for 5 days: (D) Representative photographs, (E) ear thickness and PSI score, (F) images of H&E section, (G) representative images of IHC staining of Ki-67, (H) histological analysis of epidermal thickness and (I) number of microabscesses, (J) cellular counts of cervical lymph nodes and (K) spleen weight, (L) gene expression of psoriasis-related markers in the ear skin. All the data are presented as mean ± SEM. Three to six mice per group. At least two independent experiments were performed for data analysis *in vivo*. ns, not significant, $*p < 0.05$, $**p < 0.01$, $***p < 0.001$, $****p < 0.0001$ by using one-way ANOVA with Dunnett's test compared to TYK2i-BO-gel.

the spectrum of TYK2i-BO-gel, the peaks at 2827.6 cm^{-1} and 2888.3 cm^{-1} were assigned to the alkyl groups of BO (2812.2 cm^{-1}, 2910.6 cm^{-1}). Moreover, the peak at 1652.0 cm^{-1} was assigned to the carboxyl groups of carbomer 940 (1689.8 cm^{-1}), while the peak at 1081.4 cm^{-1} was assigned to the ester bond from alginic acid (1011.6 cm^{-1}). Further, the peak at 1250.7 cm^{-1} and 670.8 cm^{-1} in the spectrum of TYK2i-BO-gel was assigned to the amide groups (1289.4 cm^{-1}) and benzene ring (655.8 cm^{-1}) of the TYK2i, respectively. Noteworthily, the molecular weight of TYK2i was not changed during the storage period (14 days) in the hydrogel (Fig. S5), indicating that the structure of TYK2i remained stable during the storage period.

2.3. Topical application of BO potentiates TYK2i in treating PsD in a preventative manner

Next, we set out to investigate the release mode of TYK2i-BO-gel in the psoriatic skin. Since the inflammatory psoriatic skin has an acidic environment with a pH around 5.0, while the pH value in the normal skin is around pH 6.0, the release rate of TYK2i from the TYK2i-BO-gel was quantified in PBS with the pH at 5.0 and 6.0 respectively [30]. As depicted in Fig. 2C, TYK2i′s release rate from the hydrogel was 26.5 % and 22.7 % in PBS at pH 5.0 and pH 6.0, respectively, after 2 h of incubation. Subsequently, the release rate of TYK2i gradually increased to 57.6 % at pH 5.0 and 60.8 % at pH 6.0 over the course of 7 days. After that, the release rate of TYK2i slowed down by 14 days of incubation at both pH levels. Notably, it is worth mentioning that the pH had a subtle impact on the drug release behavior, as evidenced by the similar release rates of TYK2i at pH 5.0 and pH 6.0. This observation suggests that the drug release occurs both in inflamed skin and during the remission stages after psoriasis treatment. Moreover, as illustrated in Fig. S6, the hemolysis test revealed outstanding hemocompatibility of TYK2i-BO-gel *in vivo*, evidenced by the minimal hemolysis rate (approaching 0 %) observed in both the vehicle-gel and TYK2i-BO-gel groups.

Next, we set out to determine whether the inclusion of BO enhanced the effectiveness of TYK2i in treating PsD. Topical corticosteroids (TC), one of the most widely used treatment modalities for psoriasis, were employed as a positive control in the following experiment. Consequently, the daily application of TYK2i-BO-gel demonstrated improvement in PsD symptoms, reaching a level comparable to that achieved by TC treatment, compared to the vehicle-gel group, as indicated by the decreased ear thickness (mean ± SEM: 0.35 ± 0.008 mm vs.0.23 ± 0.003 mm, $p < 0.0001$) and PSI (mean ± SEM: 5.9 ± 0.48 vs.1.0 ± 0.30, $p < 0.0001$) (Fig. 2D and E). Notably, the TYK2i-BO-gel treatment significantly suppressed ear edema compared to TYK2i-gel ($p = 0.039$). Histological and IHC analysis further confirmed significant reductions in the intensity of Ki-67 staining, epidermal thickness (mean ± SEM: 42.24 ± 3.09 μm vs.21.70 ± 0.68 μm, $p < 0.0001$), and counts of Munro microabcesses (mean ± SEM: 2.0 ± 0.65 vs.0.0 ± 0.0, $p = 0.005$) in mice treated with TYK2i-BO-hydrogel versus those treated with vehicle-gel (Fig. 2F–I). Similarly, decreased cellular counts of cLNs ($\times 10^6$, mean ± SEM: 9.79 ± 0.53 vs.4.33 ± 0.29, $p = 0.0001$) and a trend towards lower spleen weight (mean ± SEM: 94.40 ± 6.28 mg vs.77.80 ± 3.09 mg, $p = 0.14$) were seen in the TYK2i-BO-gel group compared to vehicle-gel group (Fig. 2J and K). The BO-loaded hydrogel alone exhibited only a modest improvement in reducing ear swelling and PSI, with minimal impact on cellular counts of cLNs and spleen size. This suggests that BO plays a subsidiary role in enhancing the anti-psoriasis effects of TYK2i. Flow cytometry analysis of ear skin demonstrated that the infiltration of neutrophils was similarly inhibited by hydrogels loaded with BO, TYK2i, or a combination of both, but TYK2i plus BO further led to a lower frequency of γδ-low T cells compared to TYK2i alone (Fig. S7). RT-PCR analysis revealed that the transcripts of *Il6*, *S100a8*, *S100a89*, and *Cxcl1* were further suppressed by the treatment of the TYK2i-BO-gel group compared to that of the TYK2i-gel or BO-gel group (Fig. 2L). To address potential safety concerns, we monitored body weight and conducted hematological and blood biochemical tests (Fig. S8). Neither IMQ

treatment alone nor in combination with vehicle-gel or TYK2i-BO-gel led to weight loss when compared with vanicream treatment. While a consecutive five-day IMQ treatment induced leukopenia in mice, subsequent application of vehicle-gel or TYK2i-BO-gel did not exacerbate the decrease in white blood cell count. No significant differences were observed among the groups receiving vanicream, IMQ, IMQ + vehicle-gel, and IMQ + TYK2i-BO-gel with respect to platelet counts (PLT), red blood cell (RBC) counts, and hemoglobin (HGB) levels. Importantly, mice treated with TYK2i-BO-gel showed no indications of hepatotoxicity, as determined by alanine transaminase (ALT) and aspartate transaminase (AST) levels, nor nephrotoxicity, as indicated by urea and creatinine (Cr) levels. Histological examinations of kidney and liver tissues also revealed no significant changes. These findings suggest that short-term topical application of TYK2i-BO-gel is not associated with overt toxicity to the blood system, liver, or kidneys. Collectively, the data demonstrated that the hydrogel formulation of TYK2i combined with BO is superior to TYK2i-loaded hydrogel in treating psoriasis in a preventative manner.

We conducted a comparative analysis of the anti-psoriasis efficacy between TYK2i-BO-gel and TYK2i-BO-oil. Topical application of vehicle-oil exacerbated PsD compared to vehicle-gel, as evidenced by measurements of ear thickness, PSI score, and the number of Munro microabscesses (Figs. S9A–D). These findings suggest that hydrogel is superior to oil as a topical drug carrier in the treatment of psoriasis. Both TYK2i-BO-gel and TYK2i-BO-oil effectively attenuated skin inflammation compared to their respective vehicle-loaded formulations. However, notably, mice treated with TYK2i-BO-gel exhibited significantly fewer psoriatic symptoms compared to those treated with TYK2i-BO-oil. Additionally, mice administered TYK2i-BO-gel showed reduced cell counts in the cLNs and less splenomegaly compared to those treated with vehicle-gel, while no significant differences were observed between the vehicle-oil and TYK2i-BO-oil treated groups (Fig. S9E). Mice treated with oil had lower body weight compared to mice treated with TYK2i-BO-gel, indicating impaired general health (Fig. S9F). Taken together, these findings suggest that TYK2i-BO-gel demonstrates superior anti-psoriasis efficacy compared to TYK2i-BO-oil.

2.4. Topical application of BO potentiates TYK2i in treating PsD in a therapeutic manner

The IMQ model, commonly used in psoriasis research, generally mimics acute skin inflammation but has limitations, such as unintended systemic effects, unclear mechanisms, and reduced suitability for chronic studies due to escalating side effects and diminishing inflammation [31]. Hydrodynamic delivery of minicircle (MC) DNA vector, which lacks bacterial DNA, achieves rapid, high-level transgene expression. Research has demonstrated that a single intravenous IL-23 MC injection induces dermatitis similar to human psoriasis, maintaining inflammation for over two months. This model allows sufficient time to assess the therapeutic efficacy of TYK2i-BO-gel on established diseases [32]. Therefore, we used the IL-23 minicircle DNA (IL-23 MC)-based murine model with features of PsD to test the effect on TYK2i-BO-gel in a therapeutic manner. We have previously demonstrated that C57BL/6 mice injected with IL-23 MC exhibited noticeable changes characterized by the presence of erythema and scaling in their ear skin as early as 5 days after delivery [32]. On day 6 post-MC delivery, mice were treated daily with vehicle-gel, BO-gel, TYK2i-gel, or TYK2i-BO-gel for 8 additional days (Fig. 3A). TYK2i-gel showed a slight improvement in the clinical phenotype, evidenced by reduced ear swelling compared to the vehicle hydrogel (Fig. 3B). However, the TYK2i-BO-gel treatment had an additional significant effect, leading to a smoother and thinner psoriatic skin appearance close to normal skin with minimal visible erythema. This treatment led to more substantial changes in ear thickness when compared to the other groups (Fig. 3C). Histologically, TYK2i-BO-gel-treated mice displayed significant reductions in epidermal thickness (mean ± SEM: GFP MC 21.94 ± 1.80
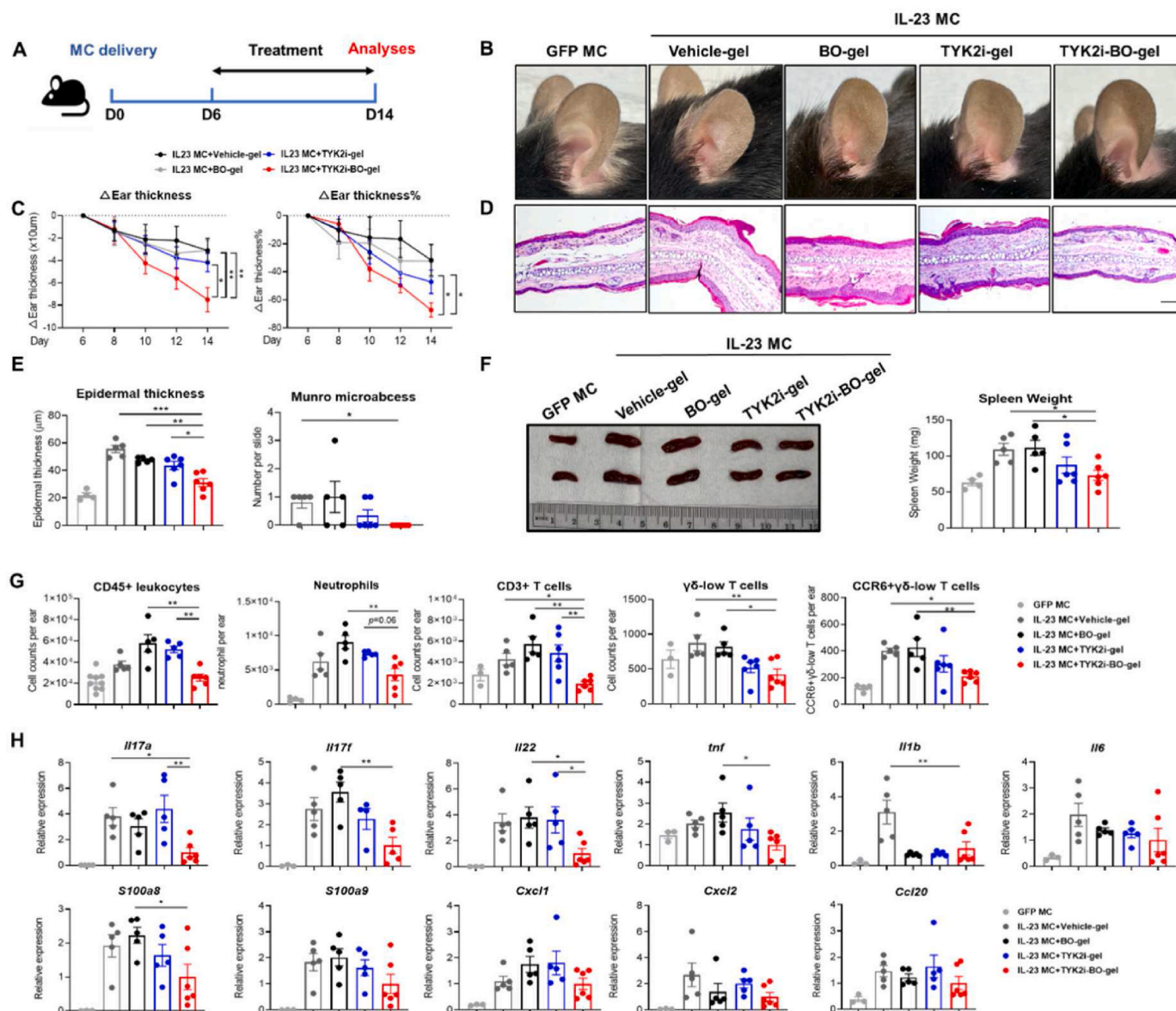
Fig. 3. Topical application of BO potentiates TYK2i in therapeutically treating PsD. (A) Schematic illustration of experimental protocols: C57BL/6 mice were treated with vehicle gel, BO-loaded gel (w/w 2 %), TYK2i-loaded gel (w/w 0.1 %), TYK2i-BO-gel (containing 0.1% TYK2i and 2% BO, w/w) for 8 consecutive days beginning at day 6 after IL-23 MC was delivered. GFP MC was delivered as control. (B) Representative photographs of the ear. (C) Absolute changes and percentage of changes in ear thickness (relative to Day 6). (D) Image of H&E section of ear skin tissue. (E) Histological analysis of epidermal thickness and number of micro-abscesses. (F) Representative images of spleen and analysis of weight. (G) Absolute numbers of CD45$^+$ leukocytes, neutrophils, CD3$^+$ T cells, γδ-low T cells, and CCR6+ γδ-low T cells in ear skin by flow cytometry. (H) Gene expression of psoriasis-related markers in the ear skin. Data were presented as fold change versus TYK2i-BO-gel. All the data were presented as mean ± SEM. Three to six mice per group. *$p < 0.05$, **$p < 0.01$, ***$p < 0.001$, by using two-way ANOVA with Turkey's multiple test in (C) and in one-way ANOVA with Dunnett's test compared to TYK2i-BO-gel (E–H).

μm, IL-23 MC + vehicle-gel 55.56 ± 2.65 μm, IL-23 MC + BO-gel 47.63 ± 0.87 μm, IL-23 MC + TYK2i-gel 43.61 ± 3.05 μm, IL-23 MC + TYK2i-BO-gel 31.14 ± 2.92 μm) and profoundly decreased numbers of Munro microabscesses compared to other groups (Fig. 3D and E). Consistent with what we observed in the IMQ-induced mice model, topical application of TYK2i-BO-gel outperformed vehicle-gel and BO-gel in efficiently attenuating splenomegaly ($p < 0.05$), indicating a suppressed status of systemic inflammation (Fig. 3F). Analysis of flow cytometry indicated that the number of total leukocytes, neutrophils, T cells, and γδ-low T cells in the ear skin, which all play a key role in the initiation and maintenance of psoriasis, were obviously suppressed by the treatment of TYK2i-BO-gel (Fig. 3G).

C–C chemokine receptor 6 (CCR6) is involved in the trafficking of IL-17-producing cells and is essential for the development of skin

inflammation in both IL-23 injection and IMQ murine PsD model [29, 33]. Our results showed that the TYK2i-BO-gel efficiently suppressed the accumulation of CCR6+ γδ-low T cells in ear skin compared to vehicle-gel ($p = 0.02$) and BO-gel ($p = 0.0093$). RT-PCR analysis revealed that treatment with the TYK2i-BO-gel resulted in a profound down-regulation in the mRNA levels of several proinflammatory markers compared to BO-gel, including *Il17f*, *tnf*, and *s100a8*. Two Th17-related markers, including *Il17a* (fold change compared to TYK2i-BO-gel, mean ± SEM: 4.40 ± 1.06 vs.1.00 ± 0.36, p = 0.007) and *Il22* (mean ± SEM: 3.61 ± 1.02 vs.1.00 ± 0.40, p = 0.05) was further suppressed by TYK2i-BO-gel relative to TYK2i-gel (Fig. 3H). Together, these results demonstrated a greater anti-psoriatic therapeutic efficiency of the TYK2i-BO hydrogel compared to the TYK2i or the BO-gel in an IL-23-mediated PsD model.

2.5. Topical administration of BO potentiates TYK2i in preventing the relapse of PsD

One of the most formidable challenges in psoriasis treatment lies in the recurrence of the disease within weeks or months following the discontinuation of the medication. Subsequently, to assess whether treatment of TYK2i-BO-gel could inhibit the recurrence of psoriasis, a modified IMQ-induced PsD model was employed (Fig. 4A) [34]. IMQ was topically applied on mouse ear skin for 3 weeks. On Day 6, inflamed skin was treated with vehicle gel, TC cream, TYK2i-gel, or TYK2i-BO-gel. Treatment was completed on Day 20, and mice were rested for 2 weeks and then rechallenged with IMQ for 4 days. Consistent with our data using the IL-23 MC model, the TYK2i-BO-gel achieved more significant therapeutic effects than the TYK2i-gel ($p = 0.0002$), where the extent of ear swelling in the TYK2i-BO-gel group was comparable to the TC group ($p = 0.92$) (Fig. 4B). Notably, despite the desired therapeutic effect of TC in skin lesions, mice receiving topical TC exhibited a greater degree of weight loss compared to the other groups (mean ± SEM: IMQ + vehicle-gel 18.38 ± 0.52 g, IMQ + TC 17.2 ± 0.43 g, IMQ + TYK2i-gel 18.66 ± 0.22 g, IMQ + TYK2i-BO-gel 18.96 ± 0.40 g) (Fig. 4C), which reflected impaired general health, possibly due to more pronounced systemic inflammation status by the treatment of the TC group. Indeed, a recent study suggested that γδ T17 cells were decreased in the skin after topical TC treatment but increased in the draining and distant LNs, potentially contributing to the recurrence of PsD upon IMQ rechallenge on the same site [34]. Upon rechallenge, mice pretreated with TC, TYK2i-gel, or TYK2i-BO-gel exhibited clinically ameliorated skin inflammation (Fig. 4D). Nevertheless, the greatest improvement, as measured by changes in the ear thickness (Day 4 after rechallenge, mean ± SEM: IMQ + vehicle-gel 0.176 ± 0.017 mm, IMQ + TC 0.067 ± 0.006 mm IMQ + TYK2i-gel 0.062 ± 0.006 mm, IMQ + TYK2i-BO-gel 0.036 ± 0.004 mm) and PSI scores (mean ± SEM: IMQ + vehicle-gel 6 ± 0.5, IMQ + TC 3.4 ± 0.37, IMQ + TYK2i-gel 3.4 ± 0.30, IMQ + TYK2i-BO-gel 1.9 ± 0.34), was seen in the TYK2i-BO-gel group (Fig. 4E). Consistently, there were more reductions in epidermal thickness (mean ± SEM: IMQ + vehicle-gel 45.89 ± 1.79 μm, IMQ + TC 33.70 ± 1.70 μm, IMQ + TYK2i-gel 37.79 ± 2.130 μm, IMQ + TYK2i-BO-gel 21.94 ± 0.28 μm) and weaker Ki-67-stained keratinocytes in the TYK2i-BO group compared to the TC or TYK2i-gel groups (Fig. 4F–H). Mice treated with TYK2i-BO-gel exhibited lower numbers of Munro microabcesses compared to the group given vehicle-gel ($p = 0.0033$) (Fig. 4I). Treatment of TC, TYK2i-gel, or TYK2i-BO-gel similarly resulted in decreased frequency and the absolute number of neutrophils and γδ-low T cells in the skin (Fig. 4J and K), while mice treated with TYK2i-BO-gel exhibited decreased numbers of leukocytes compared to those with TC ($p = 0.02$) and TYK2i-gel ($p = 0.0016$) (Fig. 4I), which might be due to lower infiltration of F4/80 positive macrophage and CD4 positive T cells (Fig. S10). No difference was noticed for the mRNA levels of pro-inflammatory markers in the ear skin among all mice after rechallenge with IMQ (Fig. S11). The high mRNA levels of cytokines might be associated with the first challenge of IMQ. Indeed, studies have proposed the concept of a residual disease gene expression profile in psoriasis, and hundreds of genes did not return to normal levels in post-treatment psoriatic lesion specimens, including those coding for proinflammatory molecules IL-22 and IL-17 [35]. Collectively, these results suggest that topical administration of TYK2i-BO-gel is more effective in
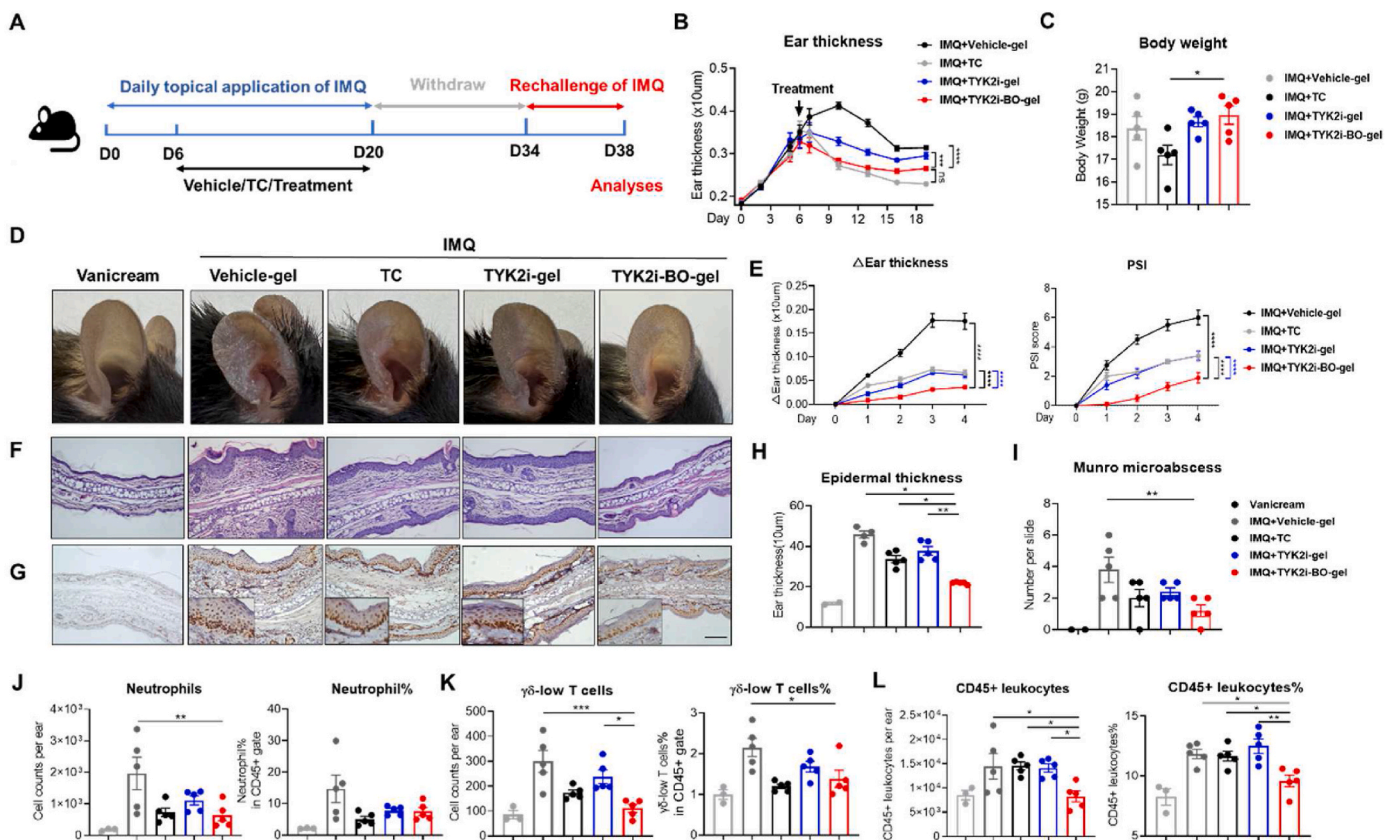
Fig. 4. Topical application of BO potentiates TYK2i in preventing the relapse of PsD. (A) Schema for mouse model establishment and treatment. (B) Ear thickness was measured from Day 0 to Day 20. (C) Body weight of mice with IMQ-induced PsD after different treatments on Day 20. (D) Representative photographs, (E) absolute changes in ear thickness (relative to day 34) and PSI scores, (F) Image of H&E section, (G) Representative images of IHC staining of Ki-67, (H) Histological analysis of epidermal thickness and (I) number of microabscesses, (J–L) Absolute numbers of CD45$^+$ leukocytes, neutrophils, and γδ-low T cells in ear skin by flow cytometry. All the data are presented as mean ± SEM. Three to five mice per group. *$p < 0.05$, **$p < 0.01$, ***$p < 0.001$, ****$p < 0.0001$ by using two-way ANOVA with Turkey's multiple test in (B, E), and one-way ANOVA with Dunnett's test compared to TYK2i-BO-gel (C, H-L).

preventing psoriatic lesion recurrence than topical TC therapy.

A long period of IMQ treatment could potentially cause adverse effects in mice [31]. We monitored body weight and conducted hematological and blood biochemical tests after 20 days of IMQ application (Fig. S12). There was no significant weight loss compared to the vanicream-treated group. Additionally, there were no signs of hepatotoxicity, as indicated by serum levels of ALT and AST, nor nephrotoxicity, as reflected by serum levels of urea and Cr. However, it is noteworthy to mention that unlike short-term applications, the 20-day IMQ treatment led to a reduction in PLT compared to the vanicream treatment.

To mitigate potential effects on the performance of the relapse PsD model resulting from reduced PLT levels in mice exposed to IMQ for 3 weeks, we made modifications by shortening the duration of the initial challenge to 1 week and prolonging the resting period to 4 weeks (Fig. S13A). The modified relapse PsD model exhibited heightened inflammation upon rechallenge. This was evidenced by more pronounced skin edema and epidermal hyperplasia, along with enhanced accumulation of total and IL-17A + producing γδ-low T cells in the skin (Figures S13 B-D). Additionally, the pretreatment of IMQ caused increased cellular counts in the cLNs, while spleen weight remained unaffected (Figures S13 E-F). We then used the modified relapse model of PsD to evaluate the potential of TYK2i-BO-gel in preventing the recurrence of psoriatic lesions. As illustrated in Fig. S14A, starting on Day 4, inflamed skin was treated with either vehicle gel or TYK2i-BO-gel for three consecutive days. During a rest period of four weeks, mice received gel treatment twice a week, a proactive therapy used clinically to prevent the relapse of inflammatory diseases [36]. Subsequently, they were rechallenged with IMQ for five days. At the end of the first

challenge (Day 7), mice treated with TYK2i-BO-gel exhibited significantly reduced ear thickness compared to those treated with vehicle-gel (Fig. S14B), consistent with our prior findings highlighting the therapeutic potential of TYK2i-BO-gel. Upon rechallenge, the TYK2i-BO-gel group displayed reduced ear skin edema, erythema, and scaling, resulting in a lower PSI score compared to the vehicle-gel group (Figs. S14C and D). Histological analysis revealed a significant decrease in epidermal thickness in the TYK2i-BO-gel group relative to the vehicle-gel group (Figs. S14E and F). Flow cytometric analysis demonstrated a reduction in the percentage of γδ-low T cells in the ear skin following treatment with TYK2i-BO-gel (Fig. S14G). Consistent with our previous findings, short-term application of IMQ resulted in leukopenia in mice compared to vanicream treatment. Pretreatment with IMQ, application of vehicle-gel or TYK2i-BO-gel did not lead to further reductions in WBC count. There were no observed differences in body weight, other hematological markers (PLT, RBC, HGB), or serum markers of liver and kidney function, among all experimental groups of mice (Figs. S14H and I). Overall, data from the modified relapse PsD model support the efficacy and safety of topical administration of TYK2i-BO-gel in preventing the recurrence of psoriatic lesions.

2.6. TYK2i-BO-gel efficiently inhibits inflammation in human psoriatic skin

As mentioned above, the IL-23 MC model (Fig. 3) primarily focuses on the IL-23/IL-17A axis, potentially limiting its utility in studying other cytokines or pathways involved in the pathogenesis of psoriasis. To further evaluate TYK2i-BO-gel's translation potential to the clinic, we assessed the effectiveness of TYK2i-BO-gel administration on human
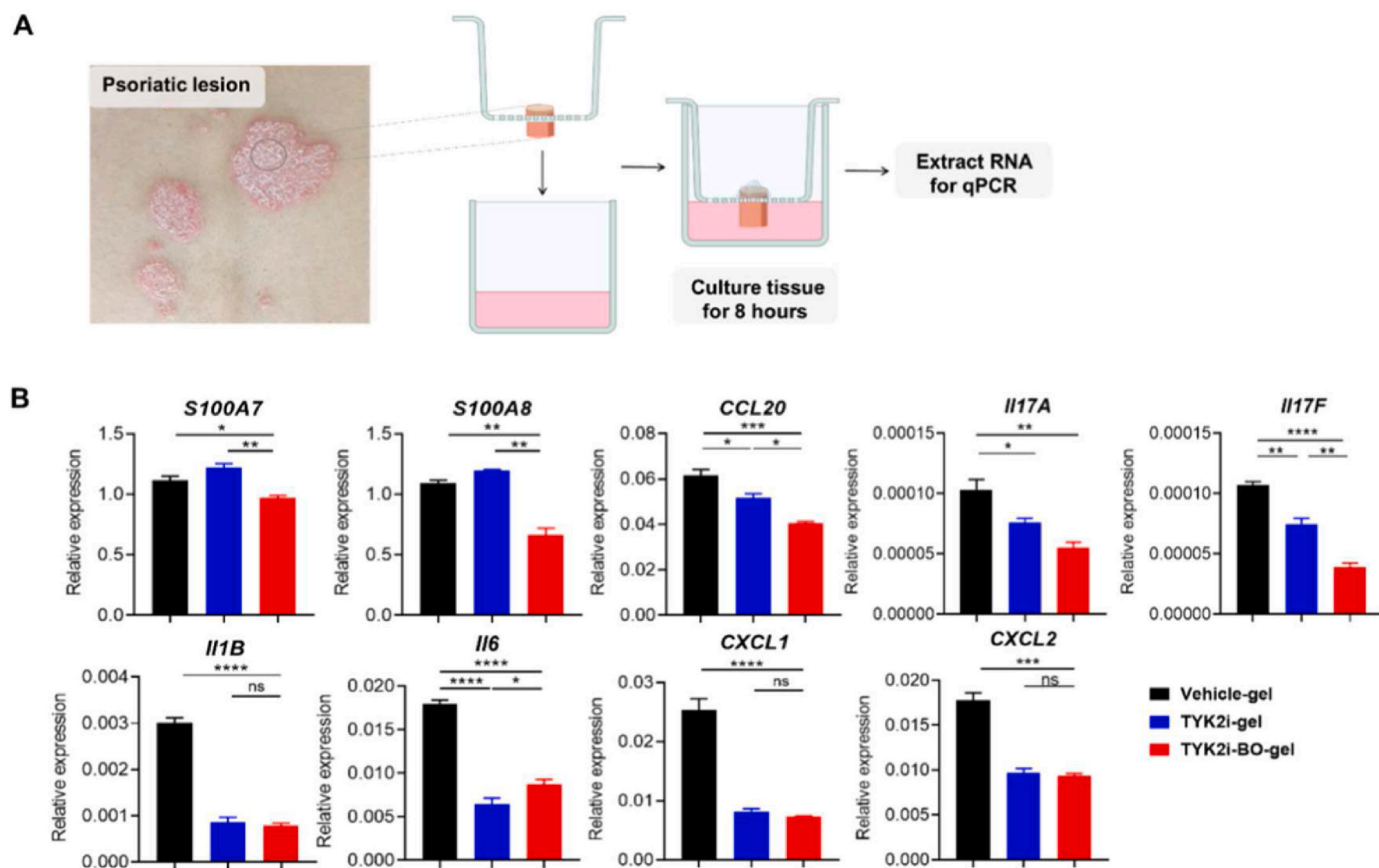

Fig. 5. BO potentiates TYK2i in suppressing inflammation in psoriatic human skin. (A) Skin biopsy from psoriatic lesion was treated with the vehicle-gel, TYK2i-gel, or TYK2i-BO-gel for 8 h and subjected to extraction of mRNA. (B) Gene expression of psoriasis-related markers in the biopsy with indicated treatment. Representative results were collected from 3 independent experiments with different donors. All the data are presented as mean ± SEM. *$p < 0.05$, **$p < 0.01$, ***$p < 0.001$, ****$p < 0.0001$ by using one-way ANOVA with Bonferroni's test.

skin samples. Biopsies were taken from the lesional psoriatic skin of patients, evenly dissected into thirds, and placed into a 6-well plate. The dissection of each biopsy was treated topically with hydrogel loaded with the vehicle, TYK2i, or TYK2i plus BO. After being maintained in culture for 8 h, RNA was isolated from the tissue and subjected to RT-PCR (Fig. 5A). Application TYK2i-gel and TYK2i-BO-gel similarly inhibited the transcripts of the pro-inflammatory markers, including *IL1B*, *IL6*, *CXCL1* and *CXCL2*. Compared to TYK2i-gel, TYK2i-BO-gel exhibited higher efficiency in suppressing Th17-related cytokines (*IL17A* and *IL17F*) and *CCL20*, a key chemokine required for blood-to-skin trafficking of IL-17-producing T cells and also for the full expression of PsD [29,37]. Notably, only TYK2i-BO-gel was capable of suppressing transcription of *S100A7* and *S100A8*, which are crucial for the dysregulated differentiation of keratinocytes [38] and inflammatory

processes in psoriatic lesion (Fig. 5B) [39]. Taken together, TYK2i-BO hydrogel demonstrated enhanced efficacy in regulating key markers of inflammation in skin explants obtained from patients with psoriasis. These findings suggest a higher therapeutic potential for TYK2i-BO-hydrogel in clinical applications for the treatment of psoriasis in human patients.

2.7. BO facilitates skin penetration of TYK2i

Building upon the potent efficacy observed in both IMQ-induced murine models and human psoriatic skin explants, we were encouraged to investigate further how BO facilitates the therapeutic effects of TYK2i in treating psoriatic inflammation. As mentioned above, BO has been identified as a potential transdermal permeation enhancer [24], so
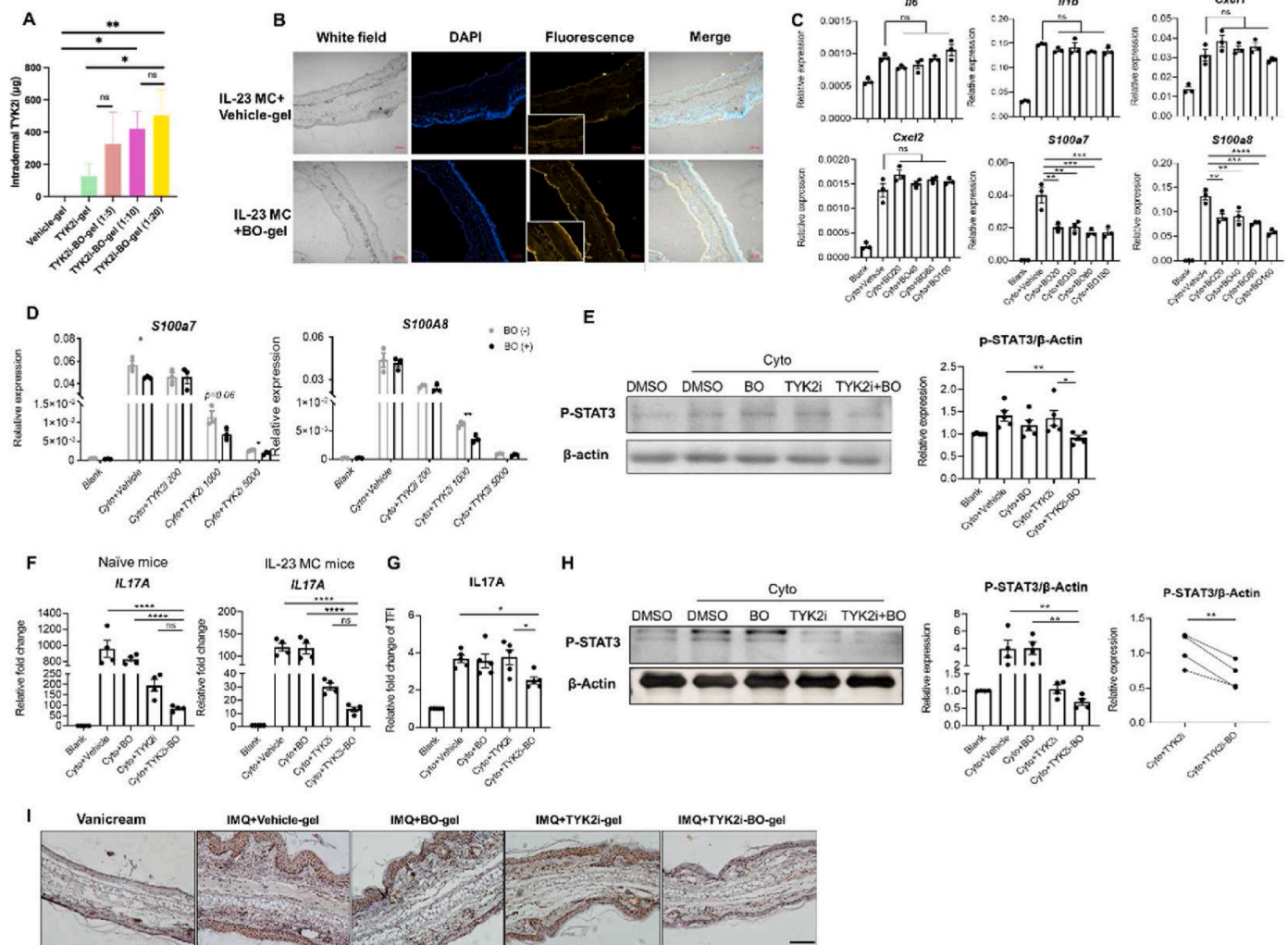
Fig. 6. BO facilitates trans-epidermal penetration and inhibits inflammation. (A) TYK2i amount in the skin after topical treatments of vehicle-gel, TYK2i-gel, and TYK2i-BO-gel for 72 h in the IL-23 MC mouse model. The ratio of TYK2i to BO was set at 1:5, 1:10, and 1:20 respectively (n = 3). The loading amount of TYK2i in the hydrogel was 1 mg in all groups. (B) Confocal images of skin penetration by gel loaded with vehicle or BO into IL-23 MC mouse psoriatic skin applied with fluorescence Rhodamine B at 24 h after administration. (C) Transcripts of psoriasis-related pro-inflammatory markers in HaCat cells co-cultured with the indicated concentrations of BO (μg/mL) in the presence of cytokine mixture stimulation. (D) Transcripts of *S100A7* and *S100A8* in HaCat cell co-culture with the indicated concentrations of TYK2i (nM) plus BO at 80 μg/mL under stimulation of cytokine mixture. (E) Effect of BO or/and TYK2i on IL-23 (50 ng/mL) and IL-1β (10 ng/mL)-induced phosphorylation of STAT3 (P-STAT3) in HaCat cells. The protein loading in all groups was normalized by co-analysis of β-Actin levels. (F) Transcripts of *IL17A* in cLN cells from naïve mice or IL-23 MC-delivered mice after 24 h of incubation in the presence of IL-23 (50 ng/mL) and IL-1β (10 ng/mL) with the vehicle, BO, TYK2i or TYK2i plus BO. (G) Relative fold change of total fluorescence intensity (TFI) of IL-17A in CD3$^+$ T cells from naïve cLN with treatment indicated. (H) Effect of BO or/and TYK2i on IL-23 (50 ng/mL) and IL-1β (10 ng/mL)-induced P-STAT3 in cLN cells. (I) Representative images of immunochemical staining of P-STAT3 from mouse ears topically treated with vanicream, IMQ plus vehicle-gel, BO-gel, TYK2i-gel or TYK2i-BO-gel. Results were collected from at least 2 independent experiments. All the data are presented as mean ± SEM. *$p < 0.05$, **$p < 0.01$, ***$p < 0.001$, ****$p < 0.0001$ by using One-way ANOVA with Turkey post hoc test in (A), one-way ANOVA with Dunnett's test compared to cytokine group in (B) or TYK2i + BO group in (D–G), two-tailed Student's t-test in (C, G).

we hypothesized that BO could potentiate TYK2i by enhancing its *trans*-epidermal delivery. To prove that, we quantified the amount of TYK2i in the skin after topical treatments of TYK2i-BO-gel with different BO contents loading in the gel for 3 days. As shown in Fig. 6A, the TYK2i amount in the skin gradually increased as the BO amount increased in the IL-23 MC mouse model. In detail, the TYK2i amount in the skin after the treatment of the TYK2i-gel group without loading BO was 124.8 ± 80.9 μg after 72 h of application. Nevertheless, the TYK2i amount in the skin after treatment of TYK2i-BO-gel (1:20) was 4-fold higher than that of the TYK2i-gel group. This result demonstrated that BO efficiently enhanced drug absorption in a dose-dependent manner. Next, to visualize the localization of TYK2i-BO-gel in the skin, we topically prepared and applied a Rhodamine B- and borneol-loaded hydrogel, *i.e.,* RhoB-BO-gel on the ear skin of IL-23 model mice, then the skin was collected on day 3 post-topical application for Cryo-section. Confocal microscopy showed that fluorescence in RhoB-BO-gel penetrated the whole epidermis, while the RhoB-gel mainly accumulated in SC (Fig. 6B), suggesting BO promoted the transdermal permeation of drugs in the psoriatic skin and would improve superior treatment efficacy of TYK2i-BO hydrogel.

Although most penetration enhancers display fairly satisfactory performance in enhancing the transdermal permeation of drug molecules across the skin, few of them have been approved for clinical application due to their skin toxicity or irritation issues. Hence, the epidermal keratinocyte HaCaT was employed to assess its toxicity on skin cells. BO at concentrations varying from 20 to 160 μg/mL did not affect the viability of keratinocytes, indicating that borneol had negligible toxicities on the epidermis (Fig. S15). Consistently, consecutive topical application of BO or BO plus TYK2i for 5 days did not induce visible signs of skin irritation (like erythema or scaling) or histopathological changes (Fig. S16).

2.8. BO potentiates the anti-inflammatory properties of TYK2i

In psoriatic lesions, activated keratinocytes can produce AMPs, cytokines, and chemokines that promote their proliferation and recruit immune cells to help initiate and reinforce inflammatory feedback loops [40]. We next examined the effects of BO on the inflammatory response of keratinocytes. Under steady status, exposure to borneol did not affect the mRNA expression of most pro-inflammatory markers on keratinocytes, except for a moderate increase in *IL1B* and *IL6* under concentrations up to 160 μg/mL (Fig. S17). We next stimulated keratinocytes with a combination of 5 cytokines (IL-17A, IL-22, IL-1α, OSM, and TNF-α) as an *in vitro* model of psoriasis [41]. A mixture of cytokines promoted the transcripts of multiple pro-inflammatory mediators in keratinocytes, among which BO profoundly suppressed the expression of AMPs, including S100A7 and S100A8 (Fig. 6C). TYK2i dampened the expression of AMP in a dose-dependent manner, and the addition of BO further inhibited their transcripts (Fig. 6D).

The transcription factor STAT3 has recently emerged as a key player in the development and pathogenesis of psoriatic inflammation [42]. Psoriatic skin exhibits elevated levels of STAT3, leading to a psoriatic phenotype in mice [43]. STAT3 is downstream of TYK2 [44], and research indicates that S100A8/S100A9 are STAT3's transcriptional targets [45]. We hypothesize that BO enhances TYK2 inhibition of AMPs by modulating STAT3 activation. As expected, the Western blot study showed that neither BO nor TYK2i dampened the levels of phosphorylated STAT3 (P-STAT3), while TYK2i-BO-gel suppressed the P-STAT3 in keratinocytes (relative fold change of intensity compared to blank, mean ± SEM: DMSO + cytokine, 1.412 ± 0.116 vs. TYK2i + BO + cytokine, 0.911 ± 0.056, *p* = 0.0083) (Fig. 6E and S18). Psoriasis is also characterized by apoptosis delay and increased proliferation of keratinocytes. However, all treatment groups showed no effects on the apoptosis and proliferation of keratinocytes (Fig. S19), suggesting that these two factors were not involved in the TYK2i-BO-gel-mediated anti-psoriasis treatment.

In psoriasis pathogenesis, IL-23 and IL-17 are considered as the key cytokines in initiating and maintaining chronic inflammation. TYK2 is the critical intracellular signal transduction link between IL-23 and IL-17. We next interrogated whether BO may assist TYK2i in inhibiting IL-17A production in T cells. Given the fact that γδ T cells rather than CD4$^+$ T cells are the predominant cellular source of IL-17A in murine models of PsD, we stimulated cLNs cells *in vitro* with IL-23 and IL-1β, two cytokines that drive differentiation of γδ17 T cells, instead of using conventional Th17 cell differentiation conditions. As expected, treatment with TYK2i significantly decreased the mRNA levels of IL-17A in cervical LN cells from both naïve mice and IL-23 MC-delivered mice. BO itself did not affect the transcripts of *IL17A* but potentiated the suppressive effect of TYK2i, as evidenced by a nearly 50 % reduction of mRNA levels in cells from the TYK2i plus BO-treated group relative to those treated with TYK2i alone (Fig. 6F). Flow cytometry confirmed the synergetic effects of BO and TYK2i by examining the protein level of IL-17A in CD3+T cells from mice cLNs (relative fold change of total fluorescence intensity (TFI) compared to blank, mean ± SEM: DMSO + cytokine, 3.661 ± 0.197 vs. TYK2i + BO + cytokine, 2.515 ± 0.183, *p* = 0.038) (Fig. 6G). Similarly, BO treatment alone did not affect the phosphorylation of STAT3 but potentiated the inhibitory effect of TYK2i (Fig. 6H and S20). Consistent with the result *in vitro*, mice ear treated with TYK2i-BO-gel exhibited weaker staining of P-STAT3 in the epidermis and cellular infiltrates in the dermis compared with those treated with vehicle-gel, BO-gel, or TYK2i-gel (Fig. 6I).

3. Conclusion

In summary, this study explored the potential of TYK2i as a topical therapy for psoriasis with the addition of BO, which had not been previously investigated. The recurrence and treatment-resistant lesions of psoriasis are major challenges in current therapies. Our study demonstrates that TYK2i-BO-gel not only matches the efficacy of TCs but also offers strong efficacy in preventing psoriasis recurrence, addressing a significant unmet medical need. The robustness and scalability of the formulation process for the topical hydrogel, combined with the use of clinically approved reagents and drugs, support the potential for future clinical translation of TYK2i-BO-loaded hydrogel as either monotherapy or an adjunct treatment for psoriasis, particularly those with resistant lesions and frequent relapses. There are two potential mechanisms accounting for the better anti-psoriatic efficacy of TYK2i-BO-gel: (1) Enhanced transdermal delivery: BO in a carbomer/alginic acid hydrogel increases skin permeability and facilitates the deeper penetration of the TYK2i into the skin layers where psoriasis inflammation occurs; (2) Synergistic effects inhibition of key cytokines and pathways: TYK2i-BO-gel inhibits the expression of AMPs in keratinocytes and suppresses the Th17 immune response, associated with the modulation of the STAT3 signaling pathway. Further studies are warranted to investigate the underlying mechanism of TYK2i-BO-gel in preventing psoriasis reoccurrence with a focus on resident memory T cells, which are considered as a major driver of psoriasis relapse [46]. To promote clinical translation, the efficacy of TYK2i-BO hydrogel should be assessed on lesions in specific body areas such as the scalp, nails, palms, soles, and intertriginous zones. Additionally, long-term toxicity studies of TYK2i-BO hydrogel *in vivo* are essential to ensure safety for clinical use. Exploring the therapeutic potential of this formulation for other inflammatory skin conditions, such as atopic dermatitis, and addressing psoriasis comorbidities, such as PsA, would also be highly beneficial.

4. Experimental section/methods

Preparation of alginic acid/carbomer hydrogel. Preparation of hydrogel matrix containing 4 % alginic acid, 1 % carbomer 940, and 5 % glycerol: The hydrogel matrix was prepared by adding 4 % alginic acid, 1 % carbomer 940, and 5 % glycerol. Briefly, 1.6 g alginic acid sodium salt (Sigma-Aldrich, Saint Louis, MO, USA) and 0.4g Carbomer 940

(Aladdin, Shanghai, China) were added into 10 mL ddH$_2$O and mixed well by sonication for 30 min. After that, the solution was reconstituted to 40 mL with ddH$_2$O. The mixed solution was allowed to stay for 2 days, and then 2 mL glycerol was added into the solution under sonication. The mixed solution was stocked at 4°C.

Preparation of cargos-loaded hydrogel. Drug loading in the alginic acid/carbomer hydrogel: For drug loading, 1 mL of the hydrogel matrix was mixed with 0.5x triethanolamine; the pH of the mixed solution was maintained at pH 7. After that, 1 mg BMS-986165 (*i.e.*, TYK2i, MCE, NJ, USA) and 20 mg Borneol (Aladdin, Shanghai, China) at a weight ratio of 1:20 were dissolved in 20 μL DMSO and were added to the matrix. The matrix was sonicated for 10 min. The prepared hydrogels were subjected to further studies. For preparing RhoB-BO-gel, the procedure was similar as mentioned above except that TYK2i was replaced with an equivalent molar quantity of Rhodamine B.

Chemical characterization of TYK2i-BO-gel. (i) FT-IR: FTIR was carried out to confirm the fabrication of TYK2i and borneol-loaded alginic acid/carbomer hydrogels. FTIR was conducted for borneol/TYK2i-loaded alginic acid/carbomer hydrogels (TYK2i-BO-gel). The samples were appropriately milled up to the desired particle size, and then FTIR (Fourier Transform Infra-Red, NICOLET 6700, Thermo Fisher, US) was used to analyze and evaluate samples. The number of scans and resolution were kept at 8 and 0.2 cm^{-1} throughout the study, respectively. FTIR spectra were kept in the range of 4000-400 cm^{-1}. **(ii) Scanning electron microscopy (SEM)** of hydrogel: The morphology and porous structure of the TYK2i-BO-hydrogel were examined using SEM -(Filed Emission Scanning Electron microscope, JSM-6330F, Japan), with an operating voltage of 15 kV. **(iii) TGA**: The degradation and thermostability of TYK2i-BO-hydrogel was detected by using a Thermogravimetric analyzer (TG209F1 Libra R).

Drug absorption study: The hydrogel was prepared as mentioned above, except that the ratio of TYK2i to BO was set at 1:5, 1:10, and 1:20 respectively. IL-23 MC model was established for 5 days and the ears of the mice were applied with (1) Vehicle gel, (2) TYK2i-gel (containing 1 mg TYK2i), (3) TYK2i-BO-gel (with a composition of 1 mg of TYK2i and 5 mg of BO), (3) TYK2i-BO-gel (with a composition of 1 mg of TYK2i and 10 mg of BO), (4) TYK2i-BO-gel (with a composition of 1 mg of TYK2i and 20 mg of BO) for 3 days (n = 3). At the end of the gel application, the mice were sacrificed and the ears were homogenized with lysis buffer. After that, the homogenizing solution was centrifuged for 10 min at a centrifuging speed set at 3000 g. The amount of TYK2i that was released in the supernatant was quantified by performing HPLC.

Stability of TYK2i during the storage period. TYK2i-BO-gel was prepared as mentioned above. 0.2 mL of the hydrogel was sampled immediately after preparation (Day 0) and again 14 days later. Each sample was mixed with 400 μL of DMSO and sonicated for 5 min to ensure complete deformation of the hydrogel. After that, the gel solution was centrifuged for 10 min at a speed of 8000 rpm. TYK2i that was released in the supernatant was collected by using the preparative RP-HPLC (Shimadzu). The molecular weight of TYK2i samples was detected by ESI mass spectra (Thermo Q-Exactive HF (High-field Orbitrap).

Release rate of TYK2i from TYK2i-BO-hydrogel: 2 copies of carbomer-alginic acid containing 1 mg TYK2i and 20 mg borneol as described above. 1 mL TYK2i-BO-Gel was immersed in 4 mL PBS at pH 5.0 and pH 6.0 respectively. At the time points of 2 h, 48 h, 72 h, day 6, and Day 14, 200 μL of supernatant was taken out and was centrifuged at a speed of 12,000 g for 10 min to remove the hydrogel fragments. The amount of TYK2i in the supernatant was analyzed by using reversed-phase high-performance liquid chromatography (RP-HPLC, Shimadzu).

Hemolysis analysis: The hemolysis rate of TYK2i-BO-gel was performed and calculated as described previously [47].

Animals: All animal experiments were performed under protocols approved by the Institutional Animal Care and Use Committee at Sun Yat-sen University (SYSU-IACUC-2023-001627) and the University of California, Davis (Protocol No: 22668). Gender and age-matched C57BL/6 mice between 8 and 12 weeks of age were purchased from the Sun Yat-sen University laboratory animal center (Guangzhou, China) or the Jackson Laboratory (Bar Harbor, ME, USA). The mice were housed, and used under pathogen-free conditions in the animal facility of Sun Yat-sen University or the University of California, Davis. All animals were randomly allocated to the individual treatment groups. For topical administration, mice were anesthetized by inhaled isoflurane. Mice were sacrificed by asphyxiation using CO$_2$ followed by cervical dislocation. Investigators were not blinded to treatment allocations, but technicians involved in assessing the clinical and histological score and sample processing were blinded. No criteria used for including and excluding animals were established a priori. We did not use statistics to predetermine sample sizes. Sample sizes in the mouse experiments were based on our experience and a pilot study with ear thickness as a primary outcome measure. The number of mice in each group was indicated in the legend.

Other experimental details including methods and supplementary figures are provided in the supplementary file.

Data availability statement

All data are available from the corresponding author by request.

Ethics approval and consent to participate

All the animal experiments were performed following the guideline approved by the Institution Animal Care and Use Committee (IACUC) at Sun Yat-sen university, Guangzhou, China (SYSU-IACUC-2023-001627) and University of California, Davis (Protocol No: 22668). Experiments involving human samples was approved by the research ethics board of Sun Yat-sen Memorial Hospital (SYSKY-2023-531-01). Informed consent of donors was obtained.

CRediT authorship contribution statement

Yuhsien Lai: Investigation, Formal analysis. **Xuesong Wu:** Investigation. **Zhuoyu Jiang:** Investigation. **Yifei Fang:** Investigation. **Xiuting Liu:** Investigation. **Dan Hong:** Investigation. **Yanyun Jiang:** Investigation. **Guozhen Tan:** Investigation. **Shiqi Tang:** Investigation. **Siyao Lu:** Investigation. **David Wei:** Writing – original draft. **Sam T. Hwang:** Writing – review & editing. **Kit S. Lam:** Writing – review & editing. **Liangchun Wang:** Investigation. **Yanyu Huang:** Writing – review & editing, Writing – original draft, Methodology, Investigation, Formal analysis, Conceptualization. **Zhenrui Shi:** Writing – review & editing, Writing – original draft, Methodology, Investigation, Funding acquisition, Formal analysis, Conceptualization.

Declaration of competing interest

The authors have no conflict of interest to declare.

Appendix A. Supplementary data

Supplementary data to this article can be found online at https://doi.org/10.1016/j.bioactmat.2024.07.013.

References

[1] C.E.M. Griffiths, A.W. Armstrong, J.E. Gudjonsson, J.N.W.N. Barker, Lancet 397 (2021) 1301–1315.
[2] J.E. Hawkes, T.C. Chan, J.G. Krueger, J. Allergy Clin. Immunol. 140 (2017) 645–653.
[3] A.W. Armstrong, C. Read, JAMA 323 (2020) 1945–1960.
[4] C.A. Elmets, N.J. Korman, E.F. Prater, E.B. Wong, R.N. Rupani, D. Kivelevitch, A. W. Armstrong, C. Connor, K.M. Cordoro, D.M.R. Davis, B.E. Elewski, J.M. Gelfand, K.B. Gordon, A.B. Gottlieb, D.H. Kaplan, A. Kavanaugh, M. Kiselica, D. Kroshinsky, M. Lebwohl, C.L. Leonardi, J. Lichten, H.W. Lim, N.N. Mehta, A.S. Paller, S. L. Parra, A.L. Pathy, M. Siegel, B. Stoff, B. Strober, J.J. Wu, V. Hariharan, A. Menter, J. Am. Acad. Dermatol. 84 (2021) 432–470.
[5] X. Hu, J. Li, M. Fu, X. Zhao, W. Wang, Signal Transduct. Targeted Ther. 6 (2021) 402.
[6] Y. Jamilloux, T. El Jammal, L. Vuitton, M. Gerfaud-Valentin, S. Kerever, P. Sève, Autoimmun. Rev. 18 (2019) 102390.
[7] A. Kvist-Hansen, P.R. Hansen, L. Skov, Dermatol. Ther. 10 (2020) 29–42.
[8] J.G. Krueger, I.B. McInnes, A. Blauvelt, J. Am. Acad. Dermatol. 86 (2022) 148–157.
[9] S.T. Wrobleski, R. Moslin, S. Lin, Y. Zhang, S. Spergel, J. Kempson, J.S. Tokarski, J. Strnad, A. Zupa-Fernandez, L. Cheng, D. Shuster, K. Gillooly, X. Yang, E. Heimrich, K.W. McIntyre, C. Chaudhry, J. Khan, M. Ruzanov, J. Tredup, D. Mulligan, D. Xie, H. Sun, C. Huang, C. D'Arienzo, N. Aranibar, M. Chiney, A. Chimalakonda, W.J. Pitts, L. Lombardo, P.H. Carter, J.R. Burke, D.S. Weinstein, J. Med. Chem. 62 (2019) 8973–8995.
[10] aA.W. Armstrong, M. Gooderham, R.B. Warren, K.A. Papp, B. Strober, D. Thaçi, A. Morita, J.C. Szepietowski, S. Imafuku, E. Colston, J. Throup, S. Kundu, S. Schoenfeld, M. Linaberry, S. Banerjee, A. Blauvelt, J. Am. Acad. Dermatol. 88 (2023) 29–39, bB. Strober, D. Thaçi, H. Sofen, L. Kircik, K. B. Gordon, P. Foley, P. Rich, C. Paul, J. Bagel, E. Colston, J. Throup, S. Kundu, C. Sekaran, M. Linaberry, S. Banerjee, K. A. Papp, J Am Acad Dermatol 2023, 88, 40-51.
[11] M.N. Landis, S.R. Smith, G. Berstein, G. Fetterly, P. Ghosh, G. Feng, V. Pradhan, S. Aggarwal, C. Banfield, E. Peeva, M.S. Vincent, J.S. Beebe, S. Tarabar, Br. J. Dermatol. 189 (2023) 33–41.
[12] T.-C. Ho, C.-C. Chang, H.-P. Chan, T.-W. Chung, C.-W. Shu, K.-P. Chuang, T.-H. Duh, M.-H. Yang, Y.-C. Tyan, Molecules 27 (2022).
[13] Y. Liang, J. He, B. Guo, ACS Nano 15 (2021) 12687–12722.
[14] aC.-Y. Chen, H. Yin, X. Chen, T.-H. Chen, H.-M. Liu, S.-S. Rao, Y.-J. Tan, Y.-X. Qian, Y.-W. Liu, X.-K. Hu, M.-J. Luo, Z.-X. Wang, Z.-Z. Liu, J. Cao, Z.-H. He, B. Wu, T. Yue, Y.-Y. Wang, K. Xia, Z.-W. Luo, Y. Wang, W.-Y. Situ, W.-E. Liu, S.-Y. Tang, H. Xie, S.J. Adv. 6 (2020) bM. Guan, G. Chu, J. Jin, C. Liu, L. Cheng, Y. Guo, Z. Deng, Y. Wang, Nanomaterials (Basel) 2022, 12; cQ. Xiao, G. Chen, Y.-H. Zhang, F.-Q. Chen, H.-F. Weng, A.-F. Xiao, Mar Drugs 2021, 19.
[15] aN. Kaur, K. Sharma, N. Bedi, Pharm. Nanotechnol. 6 (2018) 133–143, bM. T. C. P. Bernardes, S. B. N. Agostini, G. R. Pereira, L. P. da Silva, J. B. da Silva, M. L. Bruschi, R. D. Novaes, F. C. Carvalho, Eur J Pharm Sci 2021, 165, 105956; cM. Agrawal, S. Saraf, S. Saraf, S. K. Dubey, A. Puri, U. Gupta, P. Kesharwani, V. Ravichandiran, P. Kumar, V. G. M. Naidu, U. S. Murty, Ajazuddin, A. Alexander, J Control Release 2020, 327, 235-265.
[16] aY. Zhang, Y. Huang, Front. Chem. 8 (2020) 615665 bK. Y. Lee, D. J. Mooney, Prog Polym Sci 2012, 37, 106-126.
[17] M. Zhang, X. Zhao, Int. J. Biol. Macromol. 162 (2020) 1414–1428.
[18] S. Manna, P. Gupta, G. Nandi, S. Jana, J. Biomater. Sci. Polym. Ed. (2023).
[19] J. Zhang, C. Hurren, Z. Lu, D. Wang, Int. J. Biol. Macromol. 222 (2022) 1723–1733.
[20] aI.P. S. Fernando, T.U. Jayawardena, K.K.A. Sanjeewa, L. Wang, Y.-J. Jeon, W. W. Lee, Ecotoxicol. Environ. Saf. 160 (2018) 24–31, bT. U. Jayawardena, K. K. A. Sanjeewa, L. Wang, W.-S. Kim, T.-K. Lee, Y.-T. Kim, Y.-J. Jeon, Molecules 2020, 25.
[21] aR. Liu, L. Zhang, X. Lan, L. Li, T.T. Zhang, J.H. Sun, G.H. Du, Neuroscience 176 (2011) 408–419, bY. Xin, H. Zhao, J. Xu, Z. Xie, G. Li, Z. Gan, X. Wang, Carbohydr Polym 2020, 228, 115378; cS. Xiao, H. Yu, Y. Xie, Y. Guo, J. Fan, W. Yao, Bioengineered 2021, 12, 9860-9871.
[22] aS. Liu, Y. Long, S. Yu, D. Zhang, Q. Yang, Z. Ci, M. Cui, Y. Zhang, J. Wan, D. Li, A. Shi, N. Li, M. Yang, J. Lin, Pharmacol. Res. 169 (2021) 105627 bQ.-L. Zhang, B. M. Fu, Z.-J. Zhang, Drug Deliv 2017, 24, 1037-1044; cN. Chen, J. Wen, Z. Wang, J. Wang, Basic Clin Pharmacol Toxicol 2022, 130; dA. S. Sokolova, O. I. Yarovaya, D. V. Baranova, A. V. Galochkina, A. A. Shtro, M. V. Kireeva, S. S. Borisevich, Y. V. Gatilov, V. V. Zarubaev, N. F. Salakhutdinov, Arch Virol 2021, 166, 1965-1976; eR. Yuan, Y. Huang, L. Chan, D. He, T. Chen, ACS Appl Mater Interfaces 2020, 12, 45714-45727.
[23] J. Ji, R. Zhang, H. Li, J. Zhu, Y. Pan, Q. Guo, Environ. Toxicol. Pharmacol. 75 (2020) 103329.
[24] Q.-F. Yi, J. Yan, S.-Y. Tang, H. Huang, L.-Y. Kang, Drug Dev. Ind. Pharm. 42 (2016) 1086–1093.
[25] G. Aggarwal, S. Dhawan, S.L. HariKumar, Curr. Drug Deliv. 9 (2012) 172–181.
[26] M. Jabeen, A.-S. Boisgard, A. Danoy, N. El Kholti, J.-P. Salvi, R. Boulieu, B. Fromy, B. Verrier, M. Lamrayah, Pharmaceutics 12 (2020).
[27] aW.H. Lee, J.G. Rho, Y. Yang, S. Lee, S. Kweon, H.-M. Kim, J. Yoon, H. Choi, E. Lee, S.H. Kim, S. You, Y. Song, Y.S. Oh, H. Kim, H.S. Han, J.H. Han, M. Jung, Y.H. Park, Y.S. Choi, S. Han, J. Lee, S. Choi, J.-W. Kim, J.H. Park, E.K. Lee, W.K. Song, E. Kim, W. Kim, ACS Nano 16 (2022) 20057–20074, bL. van der Fits, S. Mourits, J. S. A. Voerman, M. Kant, L. Boon, J. D. Laman, F. Cornelissen, A.-M. Mus, E. Florencia, E. P. Prens, E. Lubberts, J Immunol 2009, 182, 5836-5845.
[28] M.K. Das, A.B. Ahmed, Acta Pol. Pharm. 64 (2007) 461–467.
[29] T. Mabuchi, T.P. Singh, T. Takekoshi, G.-F. Jia, X. Wu, M.C. Kao, I. Weiss, J. M. Farber, S.T. Hwang, J. Invest. Dermatol. 133 (2013) 164–171.
[30] P.L. Bigliardi, Curr. Probl. Dermatol. 54 (2018) 108–114.
[31] J.E. Hawkes, J.E. Gudjonsson, N.L. Ward, J. Invest. Dermatol. 137 (2017) 546–549.
[32] Z. Shi, E. Garcia-Melchor, X. Wu, S. Yu, M. Nguyen, D.J. Rowland, M. Huynh, T. Law, S.P. Raychaudhuri, N.L. Millar, S.T. Hwang, J. Invest. Dermatol. 140 (2020) 2386–2397.
[33] Z. Shi, E. Garcia-Melchor, X. Wu, A.E. Getschman, M. Nguyen, D.J. Rowland, M. Wilson, F. Sunzini, M. Akbar, M. Huynh, T. Law, S.K. Raychaudhuri, S. P. Raychaudhuri, B.F. Volkman, N.L. Millar, S.T. Hwang, Arthritis Rheumatol. 73 (2021) 2271–2281.
[34] N. Liu, H. Qin, Y. Cai, X. Li, L. Wang, Q. Xu, F. Xue, L. Chen, C. Ding, X. Hu, D. Tieri, E.C. Rouchka, J. Yan, J. Zheng, EBioMedicine 82 (2022) 104136.
[35] L. Puig, A. Costanzo, E.J. Muñoz-Elías, M. Jazra, S. Wegner, C.F. Paul, C. Conrad, Br. J. Dermatol. 186 (2022) 773–781.
[36] A. Lis-Święty, A. Frątczak, Dermatol. Ther. 35 (2022) e15364.
[37] M.N. Hedrick, A.S. Lonsdorf, A.-K. Shirakawa, C.-C. Richard Lee, F. Liao, S. P. Singh, H.H. Zhang, A. Grinberg, P.E. Love, S.T. Hwang, J.M. Farber, J. Clin. Invest. 119 (2009) 2317–2329.
[38] A.-K. Ekman, J. Vegfors, C.B. Eding, C. Enerbäck, Acta Derm. Venereol. 97 (2017) 441–448.
[39] H. Liang, J. Li, K. Zhang, Front. Immunol. 14 (2023) 1191645.
[40] X. Zhou, Y. Chen, L. Cui, Y. Shi, C. Guo, Cell Death Dis. 13 (2022) 81.
[41] H. Rabeony, I. Petit-Paris, J. Garnier, C. Barrault, N. Pedretti, K. Guilloteau, J.-F. Jegou, G. Guillet, V. Huguier, J.-C. Lecron, F.-X. Bernard, F. Morel, PLoS One 9 (2014) e101937.
[42] E. Calautti, L. Avalle, V. Poli, Int. J. Mol. Sci. 19 (2018).
[43] S. Sano, K.S. Chan, S. Carbajal, J. Clifford, M. Peavey, K. Kiguchi, S. Itami, B. J. Nickoloff, J. DiGiovanni, Nat. Med. 11 (2005) 43–49.
[44] E. Gracey, D. Hromadová, M. Lim, Z. Qaiyum, M. Zeng, Y. Yao, A. Srinath, Y. Baglaenko, N. Yeremenko, W. Westlin, C. Masse, M. Müller, B. Strobl, W. Miao, R.D. Inman, J. Clin. Invest. 130 (2020) 1863–1878.
[45] K. Hsu, Y.M. Chung, Y. Endoh, C.L. Geczy, PLoS One 9 (2014) e103629.
[46] D. Tian, Y. Lai, JID Innov 2 (2022) 100116.
[47] T.N. Yifei Fang, Guangze Li, Liying Wang, Jianhang Du, Jun Wu, Chem. Eng. J. 5 (2024) 147930.